The Effect of Mn Doping on the Dielectric Properties of Lead Strontium Titanate (PST)

Arne Lüker[2], Qi Zhang[1] and Paul B. Kirby[1]
[1]Materials Department, Cranfield University, Bedford
[2]Instituto Superior Técnico - Departamento de Física, Av. Rovisco Pais,Lisboa,
[1]UK
[2]Portugal

1. Introduction

Lead Strontium Titanate (PST) is a ferroelectric perovskite similar to the well known Barium Strontium Titanate (BST). Its transition point between the cubic paraelectric and tetragonal ferroelectric state (Curie temperature) can be shifted linearly by varying the Pb/Sr ratio and is just below room temperature with a ratio of 40/60. For voltage tunable applications the paraelectric state is favored because it offers low dielectric losses (tanδ) due to the absence of the permanent electric dipole, which implies that on removal of an electric field the polarization in the material returns to zero, viz. P/E measurements show no hysteresis at room temperature. The maximum tunability, defined as $n(\%) = \frac{C_{\max} - C_{\min}}{C_{\max}} \cdot 100$, where $C_{\max}$ is the capacitance value at zero bias and $C_{\min}$ the value under bias, of ferroelectrics is observed in the paraelectric state close to the Curie temperature.

At present, the research on PST thin films focuses on the diffused phase transition and relaxor behavior, the dielectric response of dc bias, and the growth kinetics on different kind of substrates and oxide buffer layers. It is commonly known that proper element doping at A or B site in ABO_3 perovskite-type ferroelectrics is an effective way to alter the ferroelectric and dielectric properties. It has been shown for BST that some dopants including Mg^{2+}, Ni^{2+}, Fe^{3+}, Mn^{2+}, Mn^{3+}, Co^{2+}, Co^{3+}, Al^{3+}, Cr^{3+} and Bi^{3+}, which can occupy the B site of the ABO_3 perovskite structure, behave as electron acceptors and can lower the dielectric loss, enhance the dielectric constant and thus the tunability and figure of merit ($FOM = \frac{n(\%)}{\tan\delta(\%)}$) [1 – 12].

For PST, being a relatively new system under increasing investigation for voltage tunable devices, only a few papers on B site doping can be found in the literature [e.g. 13 – 15] and the presented results are not very clear and satisfying. The aim of this study is to improve the material performance of PST 40/60 by doping of the B site with manganese (Mn^{2+}), which has an ionic radius of 0.67 Å, comparable to that of Ti^{4+} (0.68 Å), and was used in our lab to improve the ferroelectric and pyroelectric properties of sol-gel derived PZT tin films [16 – 18], to gain a deeper understanding of the effect of doping.

A big advantage of the sol-gel route is the ease of doping. By varying only milligrams of the dopant in the initial steps of the solution preparation, one can study the implications on the

final properties of the film time and cost effective. Starting with pure, undoped PST 40/60 we sequently increased the Mn^{2+} doping level from 1 to 5 mol% and studied the effects on morphologies, dielectric properties with and without dc bias and the ferroelectricity of the resulting thin films. It is found and explained that a doping level of 2 mol% Mn^{2+} results in optimal properties in terms of tunability and loss.

2. Experimental procedures

To prepare a 40/60 composition of (Pb,Sr) TiO_3 with, for example, 3 mol% of manganese, the stoichiometric amounts of lead acetate and strontium acetate were dissolved with slightly warming in a mixed solvent of propanediol and acetic acid. Meanwhile the stoichiometric amounts of titanium butoxide and manganese acetate were mixed in a N_2 glove box in acetic acid. Both solutions were mixed and stirred at room temperature overnight. The final solution was diluted with 2-methoxyethanol to adjust the concentration of the solution to 0.4 M.

The thus prepared precursor solution was deposited via spin coating onto silicon substrates with a Ti/Pt bottom electrode at 3000 rpm for 30 seconds. In each trial the sample was placed on a hotplate at 350°C for 10 min to evaporate the solvents and annealed on a second hotplate at 650°C for 15 min. A single layer thickness was approximately 50 nm. To obtain thicker films (~300 nm) the process was repeated six times.

An Edwards E480 thermal evaporator was used to deposit Cr/Au top electrodes onto the ferroelectric thin films through a shadow mask with hole-areas of 0.48 mm². A Siemens D5005 diffractometer was used for all the XRD measurements. Scanning electron microscopy (S-FEG SEM) was performed on a Philips XL30. To analyse the surface topography of the samples a Digital Instruments Dimension 3000 AFM was used. Contact mode was used to make high-resolution topographical images.

An RT66A Standardised Ferroelectric Test System was used to analyse the ferroelectric hysteresis properties of the thin films produced during this study.

3. Results and discussion

Fig. 1 shows X-ray diffractograms of PST 40/60 doped with 0, 1, 3 and 5 mol% Mn. All the films show a major (110) orientation at 2θ = 32.2° and are well crystallised as confirmed by SEM (Fig. 2) and AFM (Fig. 3). The SEM photographs show clearly that an increasing Mn content has a remarkable influence on the microstructure of (Pb,Sr)TiO_3. The clearly visible grains in Fig 2(a) have an average grain size of 150 nm. With increasing Mn content the grains become smaller, ~ 80 nm in 2(b), and indistinct in 2(c), and finally in 2(d), the microstructure has a sponge-like appearance.

AFM surface scans of an area of 2 x 2 µm are depicted in Fig. 3. It indicates a decrease of the RMS-roughness with increasing Mn content from 3.37 nm for pure PST down to 1.69 nm for PST with 5 mol% Mn.

The dielectric constant and loss of these films at zero bias are depicted in Fig. 4. At first the dielectric constant increases with increasing Mn content or with decreasing roughness/grain size. But there is a sharp decrease in the dielectric constant after 3 mol% Mn while the roughness/grain size is further decreasing. The dielectric constant of PST with 5 mol% Mn is even lower (~300) than that of pure PST. Sun *at al.* [19] have doped the A site of BST with K^+ and showed a clear relationship between grain size/surface roughness and

dielectricproperties of BST thin films. Both, the roughness/grain size and dielectric constant increased with the doping level up to 7.5 mol% K^+ and decreased afterwards. However, no such relationship could be found for B site Mn doped PST in this study.
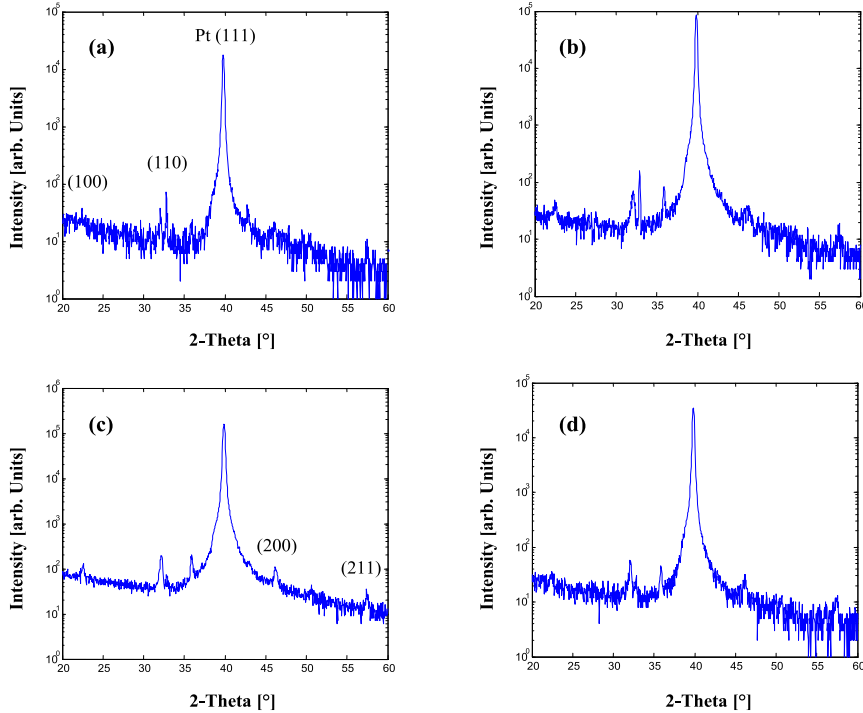

Fig. 1. X-ray diffractograms of $(Pb_{0.4},Sr_{0.6})(Ti_{1-x},Mn_x)O_3$. (a) x=0, (b) x=0.01, (c) x=0,03 and (d) x=0.05.

Li *et al.* have doped the B site of PST 40/60 with Mg^{2+} [14]. They found that the dielectric constant increases with increasing doping level up to 3 mol% Mg^{2+} with a sharp decrease afterwards. They attributed this behaviour to the generation of oxygen vacancies which induce a positive charged defect in the crystal.

Generally, oxygen vacancies are generated by heat treatment under non-oxidising atmosphere [14]. In thin films that are annealed in ambient atmosphere, they form a so-called dead-layer at the interface between the bottom electrode and the ferroelectric thin film. In the case of Mg doped PST, Mg^{2+} ions replace Ti^{4+} ions in the PST lattice due to a similar ionic radii of Mg^{2+} (r = 0.72 Å) and Ti^{4+} (r = 0.68 Å), hence B site doping. According to Li *et al.* proper Mg addition (0 < x < 0.03) in $(Pb_{0.4},Sr_{0.6})(Mg_x,Ti_{1-x})O_3$ thin films could be used as acceptors in the ABO_3 perovskite structure. It induces a negative charge and thus balances the positive of the oxygen vacancies. Then with the charge being compensated, the lattice distortion ratio in the system decreases, viz. the lattice structure of $Pb_{0.4}Sr_{0.6}Mg_xTi_{1-x}O_3$ becomes more "perfect" (cubic). According to the thermodynamic theory, the phase formation ability of the crystal therefore increases with increasing Mg content up to x = 0.03.

At the same time, more polarization paths may be provided when the lattice structure becomes more "perfect". This results in an increase of the dielectric constant.
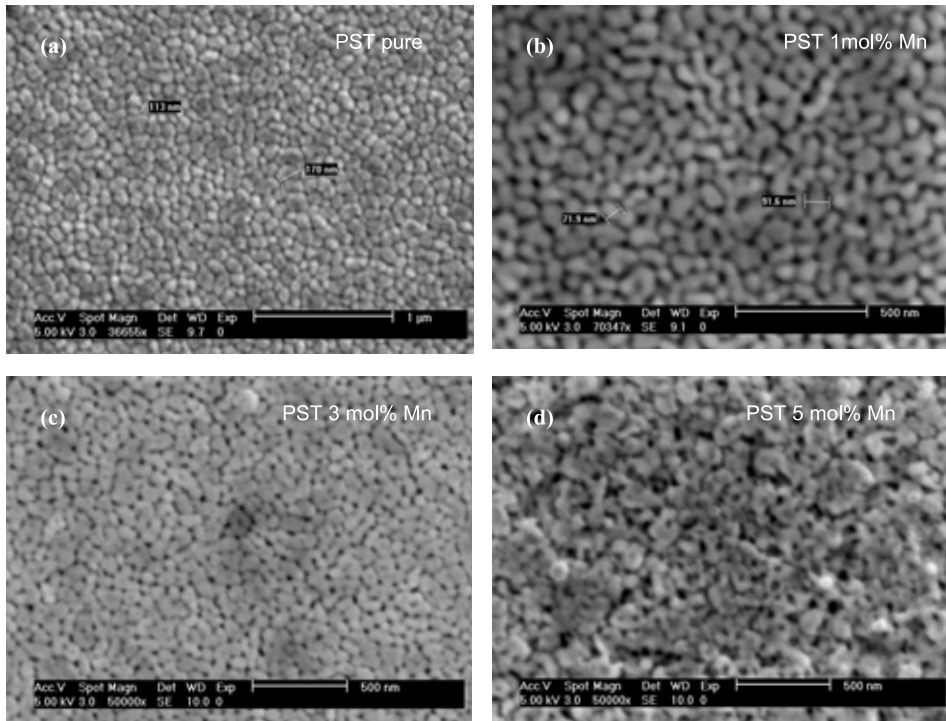

Fig. 2. SEM images of $(Pb_{0.4},Sr_{0.6})(Ti_{1-x},Mn_x)O_3$. (a) x=0, (b) x=0.01, (c) x=0,03 and (d) x=0.05

However, with further Mg doping, excessive oxygen vacancies would be created in the system. The lattice distortion ratio of the perovskite phase structure of the film would increase and then the phase formation ability decreases. The dielectric constant degrades with increasing Mg doping.

At first glance the explanation from Li *et al.* for the behaviour of the dielectric constant in Mg doped PST may as well fit for Mn doped PST. However, Mn is a multivalence ion – it can appear as Mn^{2+}, Mn^{3+} and Mn^{4+}, all having different impacts on the charge balance of the crystals. Mn^{2+} was used to improve the ferroelectric and pyroelectric properties of PZT [16 – 18] in our lab and it has been suggested that the formation of oxygen vacancies is facilitated by the conversion of Ti^{4+} to Ti^{3+} during heat treatment:

$$2Ti^{4+} \rightarrow 2Ti^{3+} + V_O^{\bullet\bullet} \text{ [1]} \tag{1}$$

---

[1] Kröger-Vink nomenclature [20]: $V_O^{\bullet\bullet}$: main character: chemical species, V=vacancy; subscript: site (for example, O=regular oxygen site); superscript: charge relative to perfect lattice; •, ', x correspond to singly positive, singly negative, and neutral effective charge.

(a)

(b)

RMS = 3.37 nm   RMS = 2.97 nm

(c)

(d)

RMS = 2.09 nm   RMS = 1.69 nm
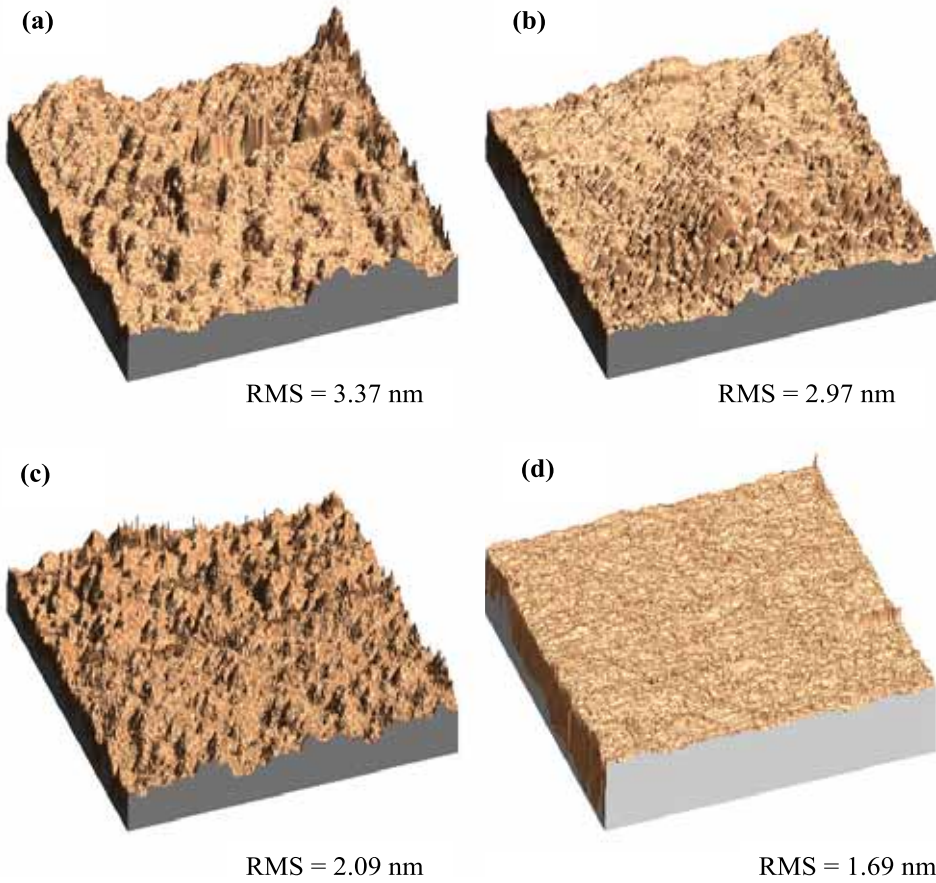
Fig. 3. AFM images of $(Pb_{0.4},Sr_{0.6})(Ti_{1-x},Mn_x)O_3$. (a) x=0, (b) x=0.01, (c) x=0,03 and (d) x=0.05. Scan size: 2*2 µm

By adding Mn^{2+} ions (and some oxygen from e.g. the atmosphere) we may find

$$\frac{1}{2}O_2 + Mn^{2+} + V_O^{\bullet\bullet} \rightarrow Mn^{4+} + O_O^X \tag{2}$$

or

$$\frac{1}{4}O_2 + Mn^{2+} + \frac{1}{2}V_O^{\bullet\bullet} \rightarrow Mn^{3+} + \frac{1}{2}O_O^X \tag{3}$$
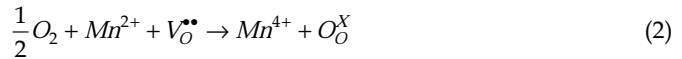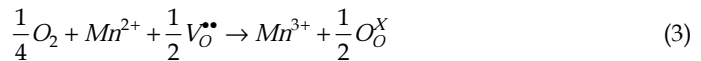
Combining these two reactions leads to two possible total reactions [21]:

$$2Ti^{4+} + Mn^{2+} + \frac{1}{2}O_2 \leftrightarrow 2Ti^{3+} + Mn^{4+} + O_O^X \tag{4}$$

or

$$2Ti^{4+} + Mn^{2+} + \frac{1}{4}O_2 \leftrightarrow 2Ti^{3+} + Mn^{3+} + \frac{1}{2}O_O^X \tag{5}$$
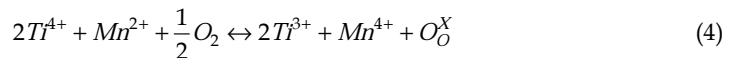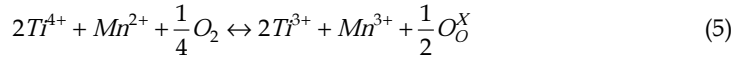
In other words: Mn^{2+} doping actually consumes oxygen vacancies to get incorporated as Mn^{3+}/Mn^{4+} at the Ti^{4+} site of the $(Pb_{0.4},Sr_{0.6})(Mn_x,Ti_{1-x})O_3$ perovskite crystal structure. It is easy to imagine that, at some point, no oxygen vacancies are available anymore. Yang *et al.* [15] doped PST 50/50 thin films with up to 5 mol% Mn and investigated the dc conductivity and the dielectric response at various temperatures. Their results reveal that there are obvious hopping conductions and dielectric relaxations at low frequencies, which can be only ascribed to the thermal-activated short range hopping of localised charge carriers through trap sites separated by potential barriers with different heights, namely, localised electron hopping between Mn^{2+}, Mn^{3+} and Mn^{4+}. They specified the activation energy for the dc-conductivity and charge carrier hopping to be 0.42 and 0.47 eV, respectively - far to low for oxygen vacancies hopping, very common in perovskite-type oxides, whose activation energy is reported to be ~1 eV [22, 23].
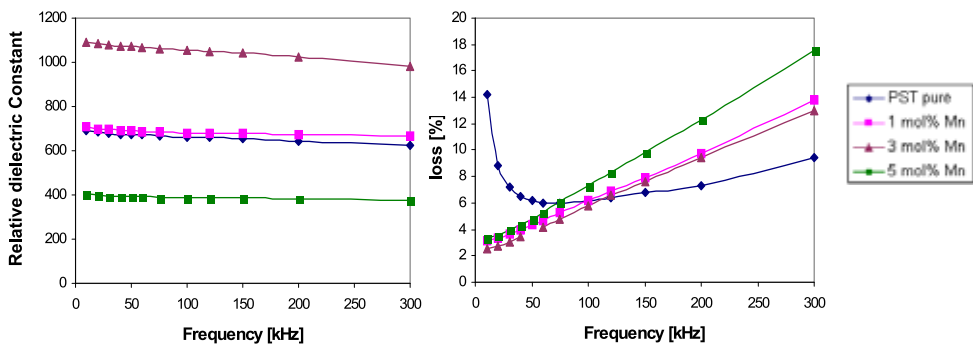

Fig. 4. Dielectric Constant and loss vs. frequency for PST 40/60 with different Mn content.

The hopping conduction due to the hopping of the charge carriers between Mn sites begins to occur in 2 mol% Mn doped PST, and then becomes distinct in 5 mol% doped films. This type of hopping process is therefore associated with a certain amount of Mn dopant and more Mn amount can provide more pathways for the total hopping process. It has been reported elsewhere that the activation energies of carrier hopping between mixed valence Mn sites are about 0.4 – 0.5 eV in Mn doped perovskite-type oxides like $LaGaO_3$ and $Bi_3PbSr_3Ca_3Cu_4O_3$ glasses [24, 25], which is in agreement with the value given by Yang *et al.*. The evidence that there are multivalence Mn ions (namely Mn^{2+}, Mn^{3+} and Mn^{4+}) in 0.2 – 1 mol% Mn doped $BaTiO_3$ has been extensively observed by electron-spin-resonance spectrum [26]. Moreover Tkach *et al.* have studied Mn-doped $SrTiO_3$ using electron paramagnetic resonance (EPR) measurements [27] and Raman spectroscopy [28]. They found that Mn^{4+} substitutes for Ti^{4+} and Mn^{2+} for Sr^{2+}. In addition they sintered $SrTi_{0.95}Mn_{0.05}TiO_3$ ceramics in O_2 and N_2 atmosphere. Sintering in O_2 favors the formation of

Mn^{4+}, whereas sintering in N_2 promotes $Mn^{2+/3+}$ on the B site, typically compensated by $V_O^{\bullet\bullet}$. However, they assumed an ionic radius of ~1.27 Å for Mn^{2+}, a value which is nearly twice as much as reported elsewhere.

For the purpose of this paper the theoretical work presented by J.Yang *et al.* is adopted and it is believed that the hopping conduction due to the hopping of the charge carriers between Mn sites lowers in the end the dielectric constant and increases the loss in PST thin films

3.1 Tunability and ferroelectricity of Mn doped PST

Fig. 5 confirms the rule of thumb for tunable ferroelectrics "a high dielectric constant gives a high tunability". It shows the tunability and loss vs. electric field at 150 kHz of $(Pb_{0.4},Sr_{0.6})(Mn_x,Ti_{1-x})O_3$ thin films with different Mn contents. The overall loss remains under 7.5 % for x = 0, 0.01, and 0.03 and increases for x = 0.05. The increase is attributed to the hopping conduction due to the hopping of the charge carriers between Mn sites, which begins to occur at x = 0.02. The tunability seems to reach a maximum of 78 % for x = 0.03 and an applied field of 350 kV/cm (10.5 V)
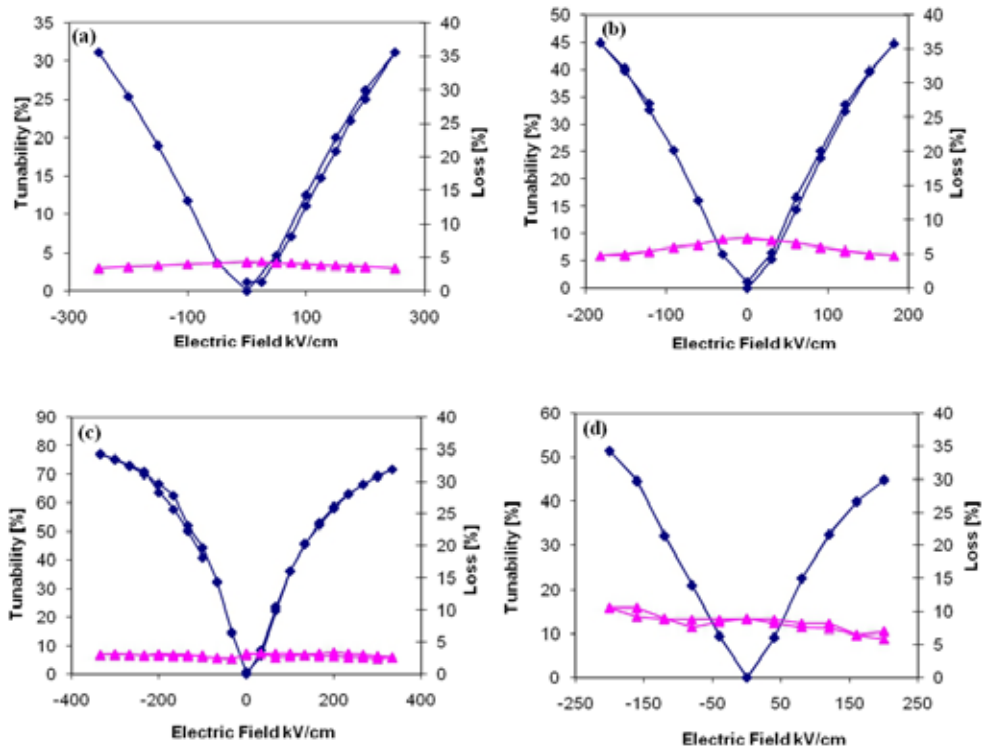

Fig. 5. Tunability and loss vs electric field at 150 kHz of $(Pb_{0.4},Sr_{0.6})(Ti_{1-x},Mn_x)O_3$. (a) x=0, (b) x=0.01, (c) x=0,03 and (d) x=0.05.

Fig. 6 compares the measured tunability with theoretical results using the expression

$$C(V) = \frac{C_{max}}{\cosh\left[\frac{2}{3}\sinh^{-1}\left(\frac{2V}{V_2}\right)\right] - 1} \tag{6}$$

for the voltage controlled capacitance [29]. C_{max} is the measured capacitance under zero bias and V_2 is the "2:1" voltage at which $C(V_2)=C_{max}/2$, normally an easily measured quantity. The figure shows that the tunability of $(Pb_{0.4},Sr_{0.6})(Mn_{0.01},Ti_{0.99})O_3$ is slightly higher than the tunability of $(Pb_{0.4},Sr_{0.6})(Mn_{0.03},Ti_{0.97})O_3$. Actually no surprise as we discovered that the hopping of the charge carriers between the Mn sites begins to occur in 2 mol% Mn doped PST. As a consequence the perovskite PST crystal is already slightly degraded at 3 mol% of Mn, as it can already be seen in Fig. 2.
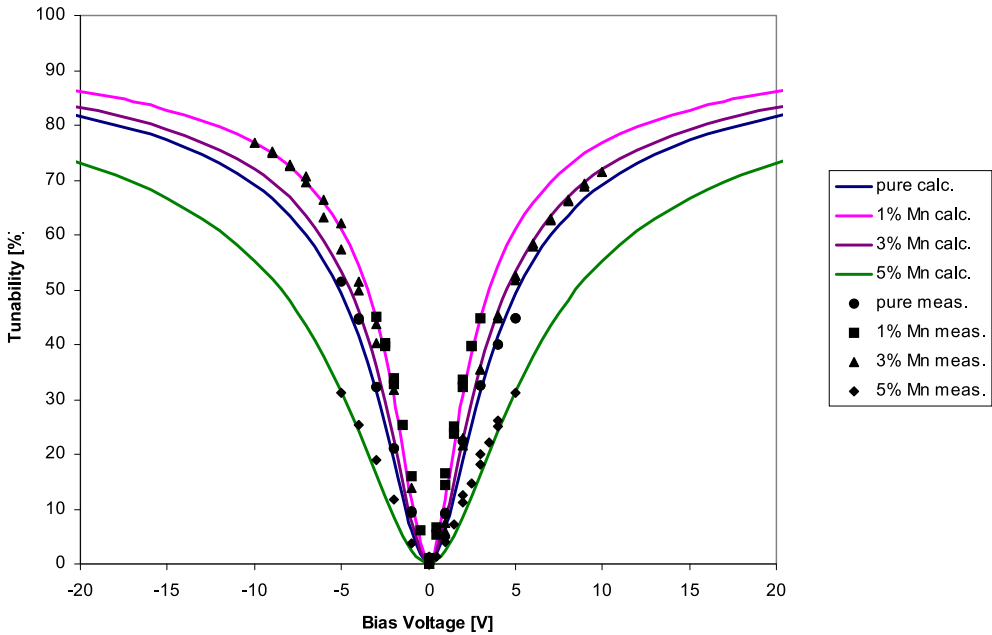

Fig. 6. Comparison of the measured and calculated tunability of $(Pb_{0.4},Sr_{0.6})(Ti_{1-x},Mn_x)O_3$. The fitting parameters $C_{max}[nF]/V_2[V]$ are: pure 9.5/5.1; 1% 15/3.5; 3% 13.8/4.5; 5% 5.7/8.5

It should be noted here that V_2 could not be measured directly for PST with 1 and 5 mol% Mn due to the early blistering of the top electrode in same cases. In these cases V_2 was calculated using the formulation

$$V_2 = \frac{4V_n}{(n+2)\sqrt{n-1}} \tag{7}$$

where V_n is the voltage at which the capacitance is reduced by n viz. $n = C_{max}/C_{min}$ [29]. The calculated curves were fitted to the values measured with positive bias because a clear relationship between Mn content and tunability can be seen within these values, whereas

the measured values for PST doped with 1 and 3 mol% are not really distinguished under negative bias.

The decrease in the oxygen vacancy concentration due to the generation of higher valance Mn ions leads as well to a restraint domain pinning, and in turn to an improvement of ferroelectric properties because oxygen vacancies are always considered as the major pinning cause of ferroelectric domain wall motions [30]. The enhancement of ferroelectric properties in $(Pb_{0.4},Sr_{0.6})(Mn_x,Ti_{1-x})O_3$ with increasing Mn content is shown in Fig. 7.

The polarisation-voltage dependence of pure PST 40/60 shows a typical paraelectric behaviour – a straight line at room temperature. With increasing Mn content both the remnant polarisation and the coercive field increase, indicating an enhancement of ferroelectricity. It should be noted here that only the first hysteresis was measured on each sample, therefore the loops are not closed.
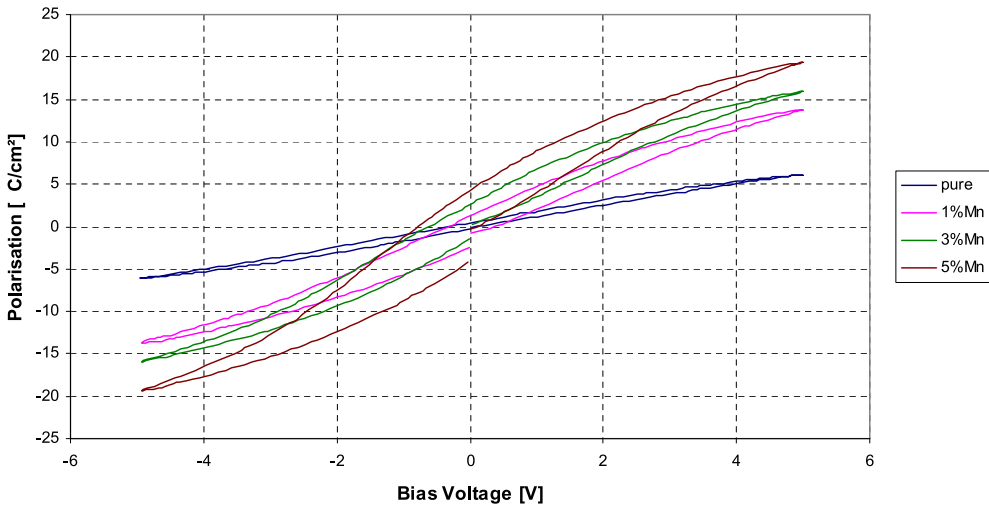

Fig. 7. Hysteresis loops of $(Pb_{0.4},Sr_{0.6})(Ti_{1-x},Mn_x)O_3$. The film is paraelectric with x=0 and the ferroelectricity improves with x.

The hysteresis loops are very slim compared to those of real ferroelectric materials like PZT and are similar to those observed in relaxor ferroelectrics in which the dielectric constant maximum does not correspond to a transition from a non-polar phase to a ferroelectric polar phase, such as observed in Lead Magnesium Niobate (PMN) [31].

On the fundamental science side it is still a challenge to develop an understanding of the many interesting and peculiar features by this kind of materials, because the interactions responsible for the relaxor ferroelectric phenomena are on the macroscopic scale. On the application side, this class of materials offers a high dielectric constant and high electrostriction, which are attractive for a broad range of devices [32].

That PST shows a relaxor behaviour was demonstrated by Hua Xu *et al*. [33] for instance. $Pb_{0.5}Sr_{0.5}TiO_3$ ferroelectric films were deposited onto $Pt/Ti/SiO_2/Si$ substrates by pulsed laser deposition. The state of the films was described as a mixed state, with both ferroelectric and relaxor-like features. The films exhibited high dielectric constant and tunability at room temperature. At 10 kHz, the dielectric constants of the 200-nm- and 400-nm-thick films were

771 and 971, with the tunability of 60.2% and 70.9%, respectively. The temperature-dependent dielectric properties were studied and the relaxor-like behavior was observed in both the thinner and thicker PST films, which could be established in terms of diffuse phase transition characteristics and Vögel–Fulcher relationship. In addition, the contribution of the film–electrode interface layer to the dielectric properties was evaluated and the true dielectric properties of the films were reconstructed. Consequently, the relaxor-like character of the PST films was mainly ascribed to the effect of the film-electrode interfaces.

4. Conclusion

Fig. 8 summarizes the main findings of this study. The dielectric constant reaches a maximum of 1100 with 3 mol% Mn; the maximum value of the tunability with 10 V is 76.72% with 1 mol% Mn and the figure of merit (FOM) reaches 23.96 with 3 mol% Mn. This compares well with results from Du *et al.* [13], who reported a tunability of 80% and a FOM of 14.17 in pure PST 40/60 and 70% and 7 in La doped PST, or Sun *et al.* [34], who achieved a tunability of 69.4% and a FOM of 28.9 in $(Pb_{0.25}Ba_{0.05}Sr_{0.7})TiO_3$.
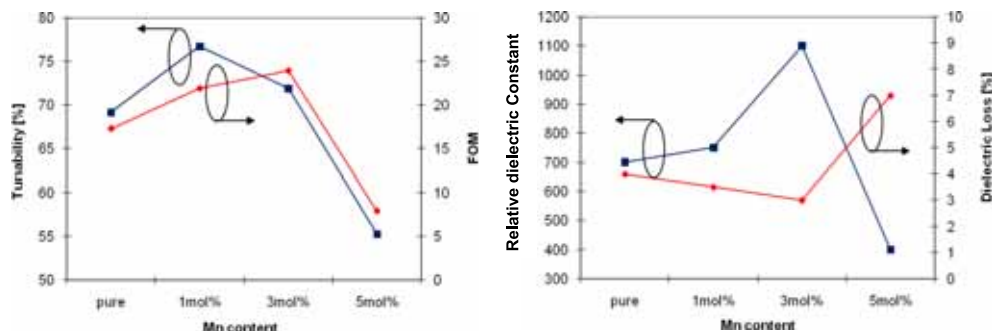

Fig. 8. Tunability and figure of merit at 10V and dielectric constant and loss at zero bias of PST 40/60 with different Mn contents

All these values drop significantly when the Mn doping level exceeds 3 mol% and we identified two possible reasons for this behaviour. First, Mn^{2+} doping consumes oxygen vacancies to get incorporated as Mn^{3+} and/or Mn^{4+} at the Ti^{4+} site of the $(Pb,Sr)TiO_3$ perovskite crystal structure. The negative charged Mn ions balance the positive induced charge of the oxygen vacancies leading to a more "perfect" (cubic) and electronically saturated perovskite. At the same time, more polarisation paths may be provided when the lattice structure becomes more "perfect". This results in an increase of the dielectric constant, tunability and FOM.

At a doping level of 2 mol% Mn, the crystal is totally saturated. With further doping a hopping conduction due to the hopping of the charge carriers between Mn sites begins to occur and becomes distinct in 5 mol% doped films. This type of hopping process is therefore associated with a certain amount of Mn dopant and more Mn amount can provide more pathways for the total hopping process. The dielectric constant, tunability and FOM decreases.

Hysteresis measurements show the effect of an enhanced ferroelectric characteristic in Mn doped PST and give rise to the question whether a relaxor like behaviour is also observable or not.

At the end it is worth pointing out that localised electron hopping between mixed-valence Mn ions provides a possibility to induce double exchange effects of Mn^{2+} and Mn^{3+} or Mn^{4+} and thus brings about magnetic properties [15]. This may be the mechanism behind the magnetic effect in Mn doped $PbTiO_3$ observed by Kumar et al. [35]. The coexisting of ferroelectric and ferromagnetic properties in a single PST thin film would provide a fresh method to obtain multiferroics.

5. Acknowledgements

6. References

M.W. Cole, C. Hubbard, E. Ngo, M. Ervin, M. Wood, and R.G. Geyer; J. Appl. Phys. 92, 475 (2002)

P.C. Joshi and M.W. Cole; Appl. Phys. Lett. 77, 289 (2000)

M.W. Cole, W.D. Nothwang, C. Hubbard, E. Ngo, and M. Ervin; J. Appl. Phys. 93, 9218 (2003)

Y.A. Jeon, T.S. Seo, and S.G. Yoon; Jpn. J. Appl. Phys., Part 1, 40, 6496 (2001)

L. Radhapiyari, A.R. James, O.P. Thakur, and C. Prakash, Mater. Sci. Eng., B 117, 5 (2005)

M. Jain, S.B. Majumder, R.S. Katiyar, F.A. Miranda, and F.W. Vam Keuls, Appl. Phys. Lett. 82, 1911 (2003)

S.Y. Wang, B.L. Cheng, C. Wang, S.Y. Dai, H.B. Lu, Y.L. Zhou, Z.H. Chen, and G.Z. Yang, Appl. Phys. Lett. 84, 4116 (2004)

S.Y. Wang, B.L. Cheng, C. Wang, H.B. Lu, Y.L Zhou, Z.H. Chen, and G.Z. Yang, J. Cryst Growth 259, 137 (2003)

K.B. Chong, L.B. Kong, L. Chen, L. Yan, C.Y. Tan, T. Yang, C.K. Ong, and T. Osipowicz, J. Appl. Phys. 95, 1416 (2004)

K.T. Kim and C.I. Kim, Thin Solid Films 472, 26 (2005)

A. Lüker, Q. Zhang, P. B. Kirby; *Thin Solid Films*, 518, 14, 3763 (2010)

D. Bhattacharyya, A. Lüker, Q. Zhang, P.B. Kirby; *Thin Solid Films*, 518, 12, 3382 (2010)

P. Du, X. Li, Y. Liu, G. Han, W. Weng; J. Europ. Ceram. Soc. 26, 2147 (2006)

X.T. Li, W.L. Huo, C.L. Mak, S. Sui, W.J. Weng, G.R. Han, G. Shen, and P.Y. Du; Mater. Chem, and Phys 108 (2008) 417 - *420*

J. Yang, X.J. Meng, M.R. Shen, L. Fang, J.L. Wang, T. Lin, J.L. Sun, and J.H. Chu, J. Appl. Phys. 104, 104113 (2008)

Q. Zhang and R.W. Whatmore, J. Appl. Phys. 94, 5228 (2003)

Q. Zhang and R.W. Whatmore, Mater. Sci. and Eng. B 109, 136 (2004)

Q. Zhang, J. Phys. D: Appl. Phys. 37, 98 (2004)

X. Sun, B. Zhu, T. Liu, M. Li and X.Z. Zhao, J. Appl. Phys. 99, 084103 (2006)

F.A. Kröger, *Chemistry of Imperfect Crystals*, North-Holland, Amsterdam, 1964

F .W.Poulsen, Solid State Ionics 129 (2000) 145– 162

N.S. Almodovar, J. Portelles, O. Raymond, J. Heiras, and J.M Siqueirosa, J. Appl. Phys. 102, 124105 (2007)

Z.H. Zhou, J.M Xue, W.Z. Li, J. Wang, H. Zhu, and J.M. Miao, J. Phys. D 38, 642 (2005)

N. Noginova, G.B. Loutts, E.S. Gillman, V.A. Atsarkin, and A.A. Verevkin, Phys. Rev. B 63, 174414 (2001)

S. Bhattacharya, D.K. Modaka, P.K. Pal, and B.K. Chaudhuri, Mater. Chem. Phys. 68, 239 (2001)

X. Wang, M. Gu,, B. Yang, S.N. Zhu, and W.W. Cao, Microelectron. Eng. 66, 855 (2003)

V. V. Laguta, I. V. Kondakova, I. P. Bykov, M. D. Glinchuk, A. Tkatch, P. M. Vilarinho; Phys. Rev. B: Condens. Matter Mater. Phys. 2007, 76, 054104

A. Tkach, P. M. Vilarinho, A. L. Kholkin, I. M. Reany, J. Pokorny, J. Petzelt; Chem. Mater. 2007, 19, 6471

A. Lüker; Sol-*Gel derived Ferroelectric Thin Films for Voltage Tunable Applications*, ISBN 978-3-639-31446-5, VDM Publishing House Ltd. (2010)

X. Wang and H. Ishiwara; Appl. Phys. Lett. 82, 2479 (2003)

G. A. Smolenskii and A. I. Agronovskaya. Sov. Phys. Tech. Phys., 3, 1380 (1958)

L. E. Cross. Ferroelectrics, 76, 29 (1987)

H. Xu, M. Shen, L. Fang, D. Yao and Z. Gan; Thin Solid Films; 493 (2005) 197

X. Sun, H. Huang, S. Wang, M. Li, and X. Zhao; Thin Solid Films 516 (2008) 1308

M. Kumar and K.L. Yadav, J. Phys.: Condens. Matter. 19, 242202 (2007)